



Data Article

Dataset of analyzes performed to determine the level and timing of selected organic pollutants' inputs in sediments of the Lake of Cavazzo (Italy)

Sarah Pizzini^{a,1}, Silvia Giuliani^{b,*}, Alina Polonia^b, Rossano Piazza^a, Luca Giorgio Bellucci^b, Beatrice Orlando^a, Andrea Gambaro^a, Luca Gasperini^b

^aDAIS-Ca¹ Foscari University of Venice, Via Torino 155, Venice Mestre (VE) I-30172, Italy

^bISMAR-CNR, Via Gobetti 101, Bologna I-40129, Italy

ARTICLE INFO

Article history:

Received 22 July 2022

Revised 12 September 2022

Accepted 19 September 2022

Available online 23 September 2022

Dataset link: [Dataset of analyzes performed to determine the level and timing of selected organic pollutants' inputs in sediments of the Lake of Cavazzo \(Italy\) \(Original data\)](#)

Keywords:

Lake of Cavazzo

Polycyclic Aromatic Hydrocarbons (PAHs)

PolyChlorinated Biphenyls (PCBs)

PolyBrominated Diphenyl Ethers (PBDEs)

OrganoChlorine Pesticides (OCPs)

Sediments

Dataset

ABSTRACT

This data article presents the dataset collected for selected organic pollutants in the framework of a larger research project aimed at assessing the effects of different environmental stressors (natural and anthropogenic) in sediments of the Lake of Cavazzo, a basin of glacial origin located in a seismically active region of the Italian Eastern Alps. Information relative to sampling strategy and operations, location of sampling sites, sedimentary chronological benchmarks, and profiles of RGB (Red-Green-Blue) color code determined from high resolution photos taken at cores CAV-04 and CAV-06 are reported, together with analytical data for 15 polycyclic aromatic hydrocarbons, 21 polychlorinated biphenyls' congeners (including the non-Aroclor CB-11), 14 polybrominated diphenyl ethers' congeners, and 22 organochlorine pesticides, whose concentrations were determined by Gas Chromatography coupled both to Low-Resolution and High-Resolution Mass Spectrometry. Interpretation of this dataset is fully discussed in the companion article by Pizzini et al. (2022) and

DOI of original article: [10.1016/j.envres.2022.113573](https://doi.org/10.1016/j.envres.2022.113573)

* Corresponding author.

E-mail address: silvia.giuliani@bo.ismar.cnr.it (S. Giuliani).

¹ Current affiliation: IRBIM-CNR, Largo Fiera della Pesca 2, I-60125, Ancona, Italy

<https://doi.org/10.1016/j.dib.2022.108633>

2352-3409/© 2022 The Authors. Published by Elsevier Inc. This is an open access article under the CC BY-NC-ND license (<http://creativecommons.org/licenses/by-nc-nd/4.0/>)

relays on the multi-proxy analysis of sediment samples presented in Polonia et al. (2021) that highlighted lake stratigraphy and major changes occurring at a decadal scale since the 1950s.

© 2022 The Authors. Published by Elsevier Inc.

This is an open access article under the CC BY-NC-ND license (<http://creativecommons.org/licenses/by-nc-nd/4.0/>)

Specifications Table

Subject	Environmental Science
Specific subject area	Environmental Chemistry Management, Monitoring, Policy, and Law Pollution
Type of data	Tables Images Figures
How the data were acquired	Color code data were determined on high resolution core pictures obtained with an Avaatech X-Ray Fluorescence (XRF) Core Scanner. Thermo Fisher Scientific Dionex ASE TM 350 (Accelerated Solvent Extractor), FMS (Fluid Management System) Power-Prep TM , and Caliper Life Science Turbopap [®] II were used for analyte extraction and pre-concentration, and extract clean-up. Single-quadrupole Low-Resolution Mass Spectrometer (LRMS) Agilent Technologies 5973 inert Mass Selective Detector System, operating in Electron Ionization mode (EI), coupled with a Gas Chromatograph (GC) Hewlett Packard - Agilent Technologies 6890 Series GC System, equipped with an Agilent Technologies HP5-ms column (30 m, 0.25 mm I.D., 0.25 µm film thickness), was used for the instrumental determination of Polycyclic Aromatic Hydrocarbons (PAHs), PolyChlorinated Biphenyls (PCBs), and OrganoChlorine Pesticides (OCPs). Double-focusing High-Resolution Mass Spectrometer (HRMS) Thermo Fisher Scientific MAT 95 XP, operating in EI mode, coupled with a GC Hewlett Packard - Agilent Technologies 6890 Series GC System, equipped with an Agilent Technologies HP5-ms column (15 m, 0.25 mm I.D., 0.25 µm film thickness), was used for the instrumental determination of PolyBrominated Diphenyl Ethers (PBDEs).
Data format	Raw Analyzed
Description of data collection	Samples for the analyzes of PAHs, PCBs, PBDEs, and OCPs were selected in order to have at least one measurement in each of the three main sedimentary units identified by Polonia et al. [2] in the sediment cores CAV-04 and CAV-06. Sediments were collected from the center of the core and far from its borders, in order to avoid any contamination from the plastic liners of the employed gravity corer.
Data source location	ISMAR-CNR (Institute of Marine Sciences-National Research Council) Via Gobetti 101, I-40129, Bologna, Italy Latitude and longitude for core CAV-04: 46.3241830169, 13.0707736704. Latitude and longitude for core CAV-06: 46.3328415174, 13.0763325040.
Data accessibility	Pizzini, Sarah; Giuliani, Silvia; Polonia, Alina; Piazza, Rossano; Bellucci, Luca Giorgio; Orlando, Beatrice; Gambaro, Andrea; Gasperini, Luca (2022), "Dataset for the DiB manuscript: Dataset of analyzes performed to determine the level and timing of selected organic pollutants' inputs in sediments of the Lake of Cavazzo (Italy)", Mendeley Data, V1. https://data.mendeley.com/datasets/7rx8hyg3dw .
Related research article	This data article is submitted as a companion paper to the research article by Pizzini et al. [1] "PAHs, PCBs, PBDEs, and OCPs trapped and remobilized in the Lake of Cavazzo (NE Italy) sediments: Temporal trends, quality, and sources in an area prone to anthropogenic and natural stressors", Environmental Research, 213 (2022) 113573. 10.1016/j.envres.2022.113573 .

Value of the Data

- Relying on the information stored in settled sediments is important when aiming at recovering reliable archives of past environmental conditions. The combination of evidences retained in sedimentary matrices with historical information relative to the industrial/urban development of a specific area can help defining responsibilities and remediation procedures.
- Sampling and analytical protocols described in this paper might inspire researchers and local administrators to develop similar studies in other problematic lacustrine areas, where natural stressors superimpose to anthropogenic impacts.
- The outcomes of further researches on longer sedimentary records and focused on the definition of wider regional sediment and water inputs could help verify the effective impact of anthropogenic stressors around the lake. Additional human actions over the area of the Lake of Cavazzo must be carefully pre-evaluated in view of this dataset and evidences from literature [1–3].
- The knowledge acquired through the study of lacustrine sedimentary records might be used to prevent future ecological crises triggered by (natural or anthropogenic) sediment remobilization.

1. Data Description

Fig. 1 depicts the study area (Lake of Cavazzo, municipalities of Cavazzo Carnico, Bordano, and Trasaghis, Friuli Venezia Giulia Region, NE Italy) and images relative to sampling operations. Fig. 1a is a georeferenced map of the lake, with the location of the two sediment cores analyzed in this paper: CAV-04 and CAV-06. Fig. 1b is a NE view of the lake where all principal human-made infrastructures are clearly visible (i.e. the A23 highway viaduct and the Somplago hydroelectric power plant on the Northern shores, the artificial outlet channel on the Southern borders of the lake). Fig. 1c shows the equipped boat used in 2015 for the seismic survey and sampling collection. Fig. 1d displays a picture of the water/sediment coring system that was used to collect the sampled sediment cores. Fig. 1e and f shows pictures of these same cores once they had been open in half, back at the laboratory of the Institute of Marine Sciences of the National Research Council (ISMAR-CNR) of Bologna.

Fig. 2 summarizes the information for the definition of sediment chronology in cores CAV-04 and CAV-06. Data are relative to the profiles of total ^{210}Pb activity ($^{210}\text{Pb}_{\text{tot}}$), logarithmic excess ^{210}Pb ($\ln ^{210}\text{Pb}_{\text{xs}}$), and ^{137}Cs activity. Pictures and radiographies of the cores are also provided, with the identification of the three main sedimentary units identified by Polonia et al. [2]. The resulting chronological benchmarks for each core are reported on the far right side of the figure, as presented in Pizzini et al. [1]. Varve count and relative formation years are provided for core CAV-06.

Fig. 3 reports color code data of the high resolution core pictures, taken by a X-Ray Fluorescence (XRF) Core Scanner, in RGB (Red-Green-Blue) values. Original sub-millimetric data (stored in the cited public repository and freely available) were averaged every 1 cm for their graphical representation. The positions of sampled layers for organic pollutants' analyzes are evidenced by black and yellow dots for cores CAV-04 (Fig. 3a) and CAV-06 (Fig. 3b), respectively.

The list of selected samples (identified by their depth in cm) for the analyzes of Polycyclic Aromatic Hydrocarbons (PAHs), PolyChlorinated Biphenyls (PCBs), PolyBrominated Diphenyl Ethers (PBDEs), and OrganoChlorine Pesticides (OCPs) is reported in Table 1. It is completed with the identification of the stratigraphic unit to which samples belong, their description, and data on ancillary parameters provided by Polonia et al. [2,3]: % sand, XRF ratios over Ti for Ca, Sr, Zr, Al, Fe, Zn, Pb, and S, $\delta^{15}\text{N}$, $\delta^{13}\text{C}$, % Total Carbon (TC), % CaCO_3 , % Total Organic Carbon (TOC), and C/N ratio.

The different steps of the analytical procedure for the analyzes of PAHs, PCBs, PBDEs, and OCPs are shown as a flow chart in Fig. 4.

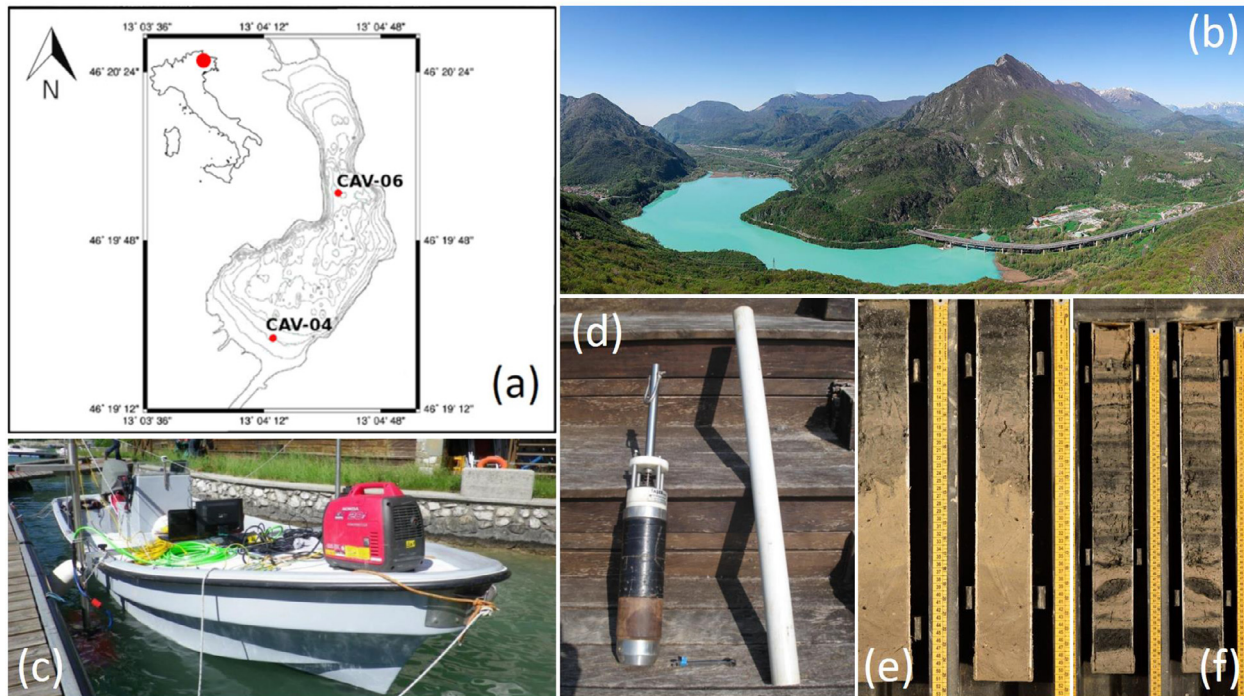


Fig. 1. Study area and sampling operations: (a) georeferenced map of the Lake of Cavazzo with the core location; (b) NE view of the lake basin (modified from © Luca De Ronch in www.sentierinatura.it) where the Somplago hydroelectric power plant and the A23 highway viaduct are visible on the lower right side of the picture; (c) the small boat used during the sampling campaign of 2015, fully equipped for seismic survey and core collection; (d) the water/sediment coring system used during the sampling campaign; (e) the two halves of core CAV-04 and (f) those of core CAV-06.

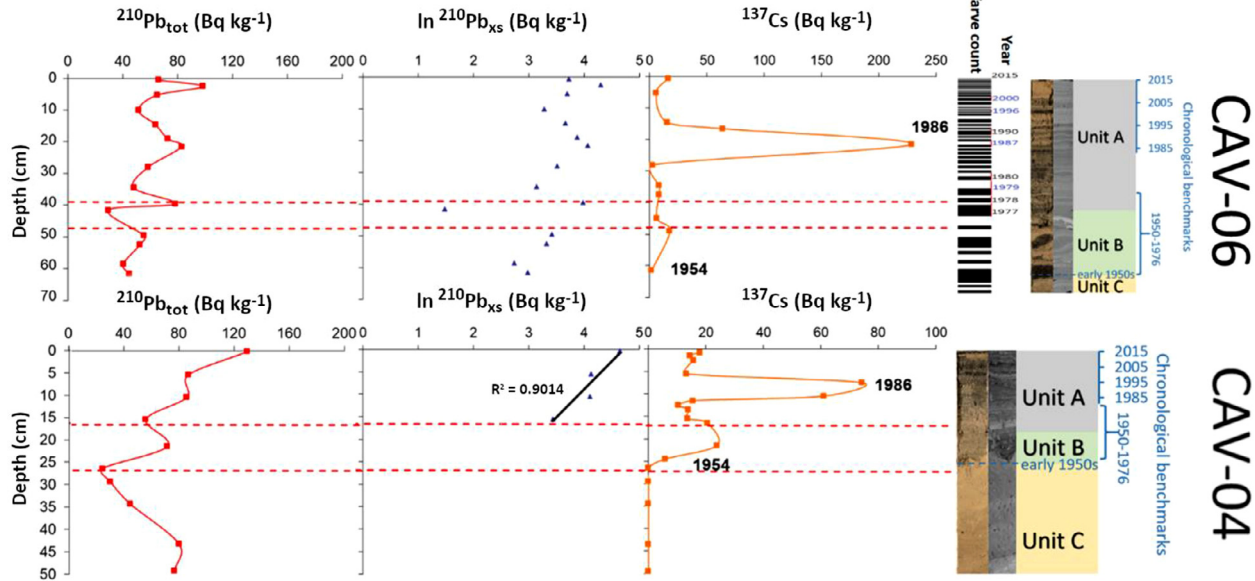


Fig. 2. Definition of sediment chronology in cores CAV-04 (below) and CAV-06 (above). Profiles of total ^{210}Pb activity ($^{210}\text{Pb}_{\text{tot}}$), logarithmic excess ^{210}Pb ($\ln ^{210}\text{Pb}_{\text{xs}}$), and ^{137}Cs activity are reported together with pictures and radiographies of the cores. The three main sedimentary units identified by Polonia et al. [2] are summarized on the right side and are accompanied by the chronological benchmarks identified for each core by Pizzini et al. [1]. The red dotted lines identify the boundaries of the sandy layer observed in both cores at different depths. Varve count and relative formation years are provided for core CAV-06. Merged and modified from Pizzini et al. [1] and Polonia et al. [2].

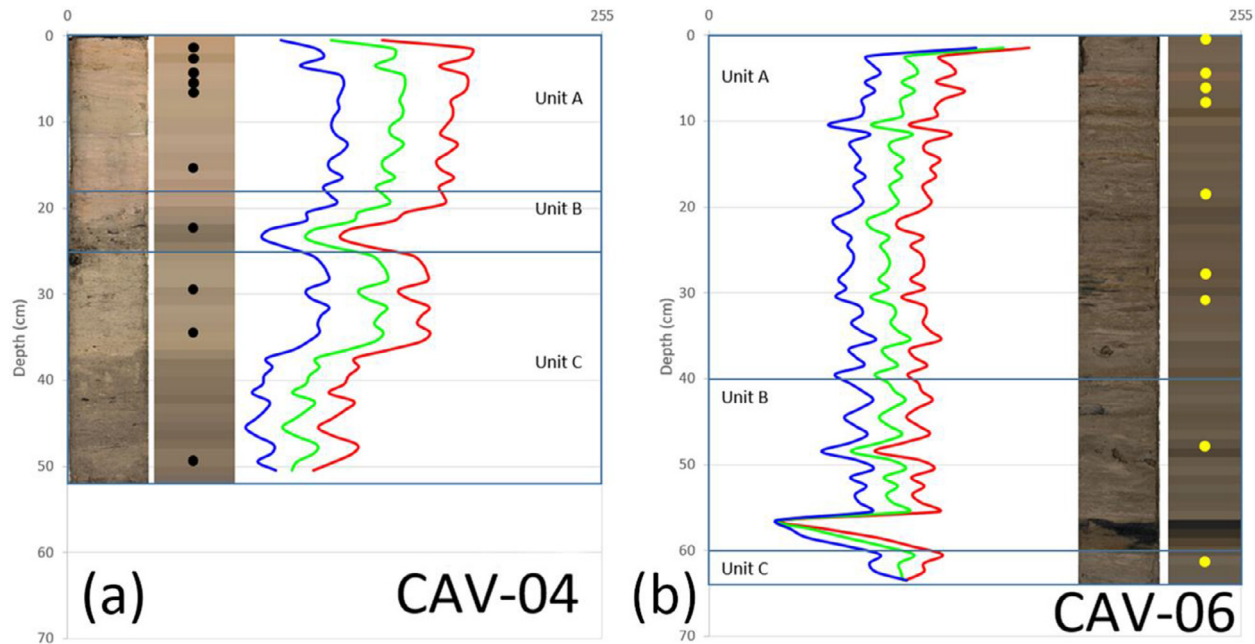


Fig. 3. Profiles of RGB (Red-Green-Blue) color code determined from high resolution photos taken by X-Ray Fluorescence (XRF) Core Scanner at cores CAV-04 (a) and CAV-06 (b). Data are averaged every 1 cm. Original sub-millimetric values are stored in the cited public repository and are freely available. High resolution photos and their relative graphical representations are also shown. The positions of sampled layers for organic pollutants' analyses are evidenced by colored dots (black for core CAV-04, yellow for core CAV-06).

Table 1

List of selected samples for the analyzes of PAHs, PCBs, PBDEs, and OCPs, with their description and ancillary data provided by Polonia et al. [2,3].

Core	Level (cm)	Stratigraphic unit	Description of layer	% sand	Ca/Ti	Sr/Ti	Zr/Ti	Al/Ti	Fe/Ti	Zn/Ti	Pb/Ti	S/Ti	$\delta^{15}\text{N}$	$\delta^{13}\text{C}$	% TC	% CaCO_3	% TOC	C/N
CAV-04	1-2	A	undisturbed	9.4	113	4.47	0.76	0.69	13.7	0.23	0.14	0.27	1.11	-26.9	7.67	56.7	0.87	10.2
	2-3	A	dark	23	98.5	4.87	0.76	0.56	13.5	0.22	0.14	0.41	0.49	-27.3	7.61	54.4	1.07	9.88
	4-5	A	light	7.2	87.0	4.86	0.86	0.54	14.8	0.24	0.16	0.53	1.73	-26.5	8.13	62.4	0.63	13.5
	5-6	A	dark	6.0	90.6	4.20	0.82	0.52	14.0	0.24	0.17	0.40	n.a.	n.a.	n.a.	n.a.	n.a.	n.a.
	6-7	A	light	9.7	105	5.51	0.89	0.58	15.8	0.27	0.21	0.55	n.a.	n.a.	n.a.	n.a.	n.a.	n.a.
	15-16	A	light	21	108	6.08	1.23	0.32	16.3	0.44	0.32	0.91	2.86	-25.6	7.59	55.1	0.98	15.7
	21-22	B	coarser	57	202	4.17	0.77	0.66	15.4	0.36	0.41	1.30	n.a.	n.a.	n.a.	n.a.	2.61	n.a.
	29-30	C		25	3055	25.58	4.78	0.82	46.0	1.55	1.52	6.18	2.53	-27.7	12.5	89.8	1.72	14.3
	34-35	C		18	5185	39.87	7.00	2.31	68.7	2.38	2.64	6.95	2.39	-27.9	12.7	93.4	1.46	12.4
	49-50	C	bottom	18	1322	11.55	2.99	0.92	23.7	0.74	0.59	0.08	3.13	-27.6	12.7	91.6	1.70	15.4
CAV-06	0-1	A	top	2.2	76.2	2.98	0.89	0.56	12.7	0.26	0.21	0.51	2.34	-26.8	6.47	47.1	0.82	13.8
	4.5-6	A	light	2.6	43.0	1.80	0.76	0.41	12.6	0.19	0.15	0.34	1.47	-27.2	6.40	47.9	0.65	9.90
	6-7	A	dark	2.4	74.5	3.01	0.96	0.33	13.9	0.25	0.34	0.57	2.04	-26.8	3.44	25.7	0.35	7.71
	7.5-8.5	A	light	2.8	82.6	2.77	0.88	0.36	13.1	0.23	0.18	0.52	-0.70	-27.1	8.61	66.6	0.61	4.09
	9.5-10.5	A	dark	3.2	65.0	2.11	0.71	0.56	11.7	0.21	0.19	0.35	1.60	-27.4	8.00	61.0	0.68	10.1
	18.5-19.5	A	light	3.6	57.9	2.84	0.97	0.29	14.0	0.28	0.22	0.58	0.73	-27.6	8.69	61.9	1.55	18.6
	27.5-28.5	A	dark	4.8	73.0	2.94	1.01	0.28	15.6	0.34	0.24	0.86	1.42	-27.3	8.56	60.0	1.66	16.1
	31-32	A		3.0	70.9	2.95	1.05	0.31	12.1	0.27	0.21	0.65	1.33	-26.5	7.03	53.9	0.56	10.7
	48-50	B	dark	6.7	77.6	3.86	1.28	0.44	15.5	0.38	0.28	0.84	1.10	-26.6	8.53	54.0	2.04	21.8
	61-62	C	bottom	2.0	68.0	3.47	1.11	0.36	14.0	0.42	0.36	0.57	2.04	-26.3	7.94	60.2	0.71	16.8

TC = Total Carbon; TOC = Total Organic Carbon.

n.a. = not available.

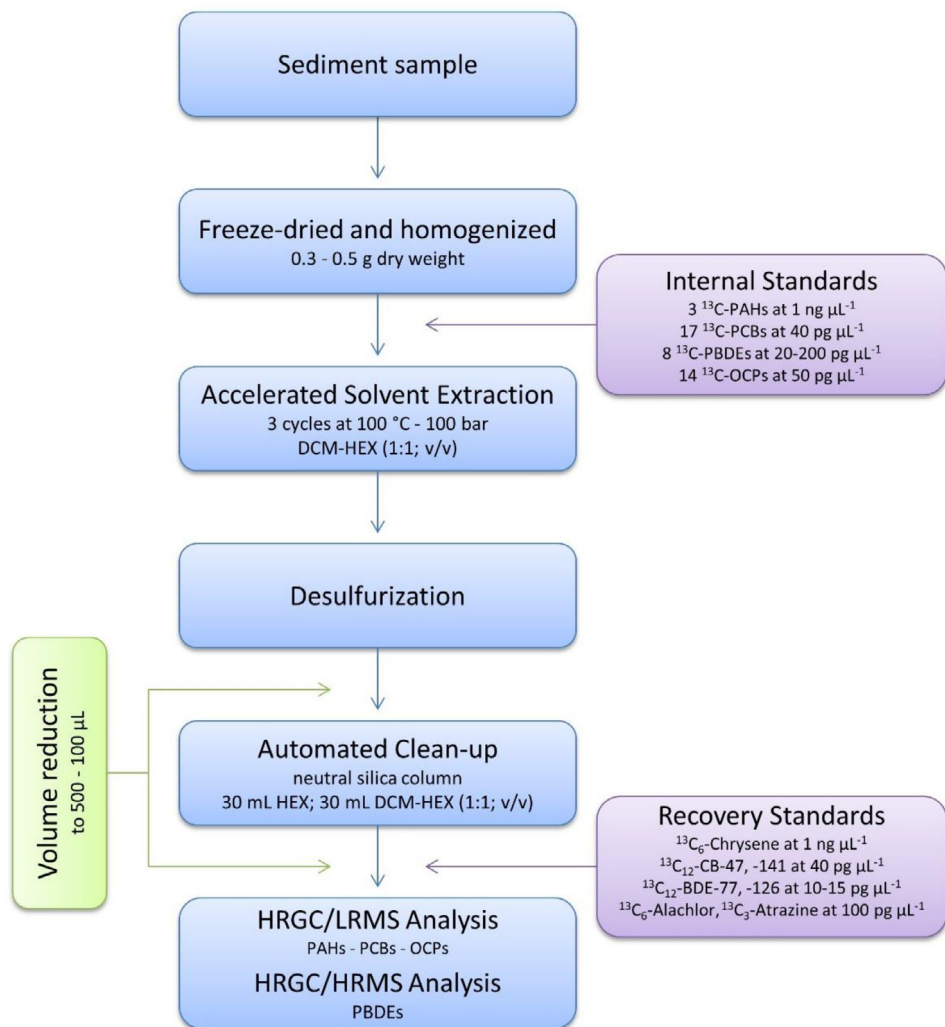


Fig. 4. Flow chart of the analytical procedure used for the determination of PAHs, PCBs, PBDEs, and OCPs. DCM = dichloromethane; HEX = *n*-hexane; HRGC = High-Resolution Gas Chromatograph; LRMS = Low-Resolution Mass Spectrometer; HRMS = High-Resolution Mass Spectrometer.

All internal quantification standards and internal recovery standards (i.e. the ^{13}C isotope-labeled compounds presented in Fig. 4) used during the analyzes are summarized in Table 2.

Tables 3–6 show the operating conditions and the instrumental parameters set for the determination of PAHs, PCBs, PBDEs, and OCPs, respectively.

Tables 7 report the class of chlorination/bromination, the congener number, and IUPAC (International Union of Pure and Applied Chemistry) name of the 21 PCBs and 14 PBDEs analyzed by Pizzini et al. [1], respectively.

Tables 9–12 and 8 displays the data relative to the measured concentrations (in ng g^{-1}) of the pollutants analyzed by Pizzini et al. [1]. Method Detection Limits (MDLs; in ng g^{-1}) are also reported. Table 9 refers to PAHs, Table 10 to PCBs, Table 11 to PBDEs, and Table 12 to OCPs.

Table 2

List of the ^{13}C isotope-labeled compounds used as internal quantification standards and internal recovery standards for the analyzed 15 PAHs, 21 PCBs, 14 PBDEs, and 22 OCPs.

Class	Analyte	Internal quantification standard	Internal recovery standard
PAHs	Acenaphthylene	$^{13}\text{C}_6$ Acenaphthylene*	$^{13}\text{C}_6$ Chrysene*
	Acenaphthene	$^{13}\text{C}_6$ Acenaphthylene*	$^{13}\text{C}_6$ Chrysene*
	Fluorene	$^{13}\text{C}_6$ Acenaphthylene*	$^{13}\text{C}_6$ Chrysene*
	Phenanthrene	$^{13}\text{C}_6$ Phenanthrene*	$^{13}\text{C}_6$ Chrysene*
	Anthracene	$^{13}\text{C}_6$ Phenanthrene*	$^{13}\text{C}_6$ Chrysene*
	Fluoranthene	$^{13}\text{C}_6$ Phenanthrene*	$^{13}\text{C}_6$ Chrysene*
	Pyrene	$^{13}\text{C}_6$ Phenanthrene*	$^{13}\text{C}_6$ Chrysene*
	Benzo[a]anthracene	$^{13}\text{C}_6$ Phenanthrene*	$^{13}\text{C}_6$ Chrysene*
	Chrysene	$^{13}\text{C}_6$ Phenanthrene*	$^{13}\text{C}_6$ Chrysene*
	Benzo[b]fluoranthene	$^{13}\text{C}_6$ Benzo[a]pyrene*	$^{13}\text{C}_6$ Chrysene*
	Benzo[k]fluoranthene	$^{13}\text{C}_6$ Benzo[a]pyrene*	$^{13}\text{C}_6$ Chrysene*
	Benzo[a]pyrene	$^{13}\text{C}_6$ Benzo[a]pyrene*	$^{13}\text{C}_6$ Chrysene*
	Benzo[ghi]perylene	$^{13}\text{C}_6$ Benzo[a]pyrene*	$^{13}\text{C}_6$ Chrysene*
	Indeno[1,2,3-cd]pyrene	$^{13}\text{C}_6$ Benzo[a]pyrene*	$^{13}\text{C}_6$ Chrysene*
	Dibenz[a,h]anthracene	$^{13}\text{C}_6$ Benzo[a]pyrene*	$^{13}\text{C}_6$ Chrysene*
	PCBs	CB-11	$^{13}\text{C}_{12}$ CB-15*
CB-29		$^{13}\text{C}_{12}$ CB-28*	$^{13}\text{C}_{12}$ CB-47*
CB-31,28		$^{13}\text{C}_{12}$ CB-28*	$^{13}\text{C}_{12}$ CB-47*
CB-52		$^{13}\text{C}_{12}$ CB-52*	$^{13}\text{C}_{12}$ CB-47*
CB-81		$^{13}\text{C}_{12}$ CB-81*	$^{13}\text{C}_{12}$ CB-47*
CB-77		$^{13}\text{C}_{12}$ CB-77*	$^{13}\text{C}_{12}$ CB-47*
CB-101,90		$^{13}\text{C}_{12}$ CB-118*	$^{13}\text{C}_{12}$ CB-141*
CB-123		$^{13}\text{C}_{12}$ CB-123*	$^{13}\text{C}_{12}$ CB-141*
CB-118		$^{13}\text{C}_{12}$ CB-118*	$^{13}\text{C}_{12}$ CB-141*
CB-114		$^{13}\text{C}_{12}$ CB-114*	$^{13}\text{C}_{12}$ CB-141*
CB-105		$^{13}\text{C}_{12}$ CB-105*	$^{13}\text{C}_{12}$ CB-141*
CB-126		$^{13}\text{C}_{12}$ CB-126*	$^{13}\text{C}_{12}$ CB-141*
CB-153		$^{13}\text{C}_{12}$ CB-153*	$^{13}\text{C}_{12}$ CB-141*
CB-164,138		$^{13}\text{C}_{12}$ CB-153*	$^{13}\text{C}_{12}$ CB-141*
CB-128,167		$^{13}\text{C}_{12}$ CB-167*	$^{13}\text{C}_{12}$ CB-141*
CB-156		$^{13}\text{C}_{12}$ CB-156*	$^{13}\text{C}_{12}$ CB-141*
CB-157		$^{13}\text{C}_{12}$ CB-157*	$^{13}\text{C}_{12}$ CB-141*
CB-169		$^{13}\text{C}_{12}$ CB-169*	$^{13}\text{C}_{12}$ CB-141*
CB-185	$^{13}\text{C}_{12}$ CB-180*	$^{13}\text{C}_{12}$ CB-141*	
CB-180	$^{13}\text{C}_{12}$ CB-180*	$^{13}\text{C}_{12}$ CB-141*	
CB-189	$^{13}\text{C}_{12}$ CB-189*	$^{13}\text{C}_{12}$ CB-141*	
PBDEs	BDE-17	$^{13}\text{C}_{12}$ BDE-28*	$^{13}\text{C}_{12}$ BDE-77*
	BDE-28	$^{13}\text{C}_{12}$ BDE-28*	$^{13}\text{C}_{12}$ BDE-77*
	BDE-71	$^{13}\text{C}_{12}$ BDE-47*	$^{13}\text{C}_{12}$ BDE-77*
	BDE-47	$^{13}\text{C}_{12}$ BDE-47*	$^{13}\text{C}_{12}$ BDE-77*
	BDE-66	$^{13}\text{C}_{12}$ BDE-47*	$^{13}\text{C}_{12}$ BDE-77*
	BDE-100	$^{13}\text{C}_{12}$ BDE-100*	$^{13}\text{C}_{12}$ BDE-126*
	BDE-99	$^{13}\text{C}_{12}$ BDE-99*	$^{13}\text{C}_{12}$ BDE-126*
	BDE-85	$^{13}\text{C}_{12}$ BDE-100*	$^{13}\text{C}_{12}$ BDE-126*
	BDE-154	$^{13}\text{C}_{12}$ BDE-154*	$^{13}\text{C}_{12}$ BDE-126*
	BDE-153	$^{13}\text{C}_{12}$ BDE-153*	$^{13}\text{C}_{12}$ BDE-126*
	BDE-138	$^{13}\text{C}_{12}$ BDE-154*	$^{13}\text{C}_{12}$ BDE-126*
	BDE-183	$^{13}\text{C}_{12}$ BDE-183*	$^{13}\text{C}_{12}$ BDE-126*
	BDE-190	$^{13}\text{C}_{12}$ BDE-183*	$^{13}\text{C}_{12}$ BDE-126*
	BDE-209	$^{13}\text{C}_{12}$ BDE-209*	$^{13}\text{C}_{12}$ BDE-126*

(continued on next page)

Table 2 (continued)

Class	Analyte	Internal quantification standard	Internal recovery standard
OCPs	Pentachlorobenzene	¹³ C ₆ Hexachlorobenzene*	¹³ C ₃ Atrazine
	Hexachlorobenzene	¹³ C ₆ Hexachlorobenzene*	¹³ C ₃ Atrazine
	α-HCH	¹³ C ₆ α-HCH*	¹³ C ₃ Atrazine
	β-HCH	¹³ C ₆ β-HCH*	¹³ C ₃ Atrazine
	γ-HCH	¹³ C ₆ γ-HCH*	¹³ C ₃ Atrazine
	δ-HCH	¹³ C ₆ γ-HCH*	¹³ C ₃ Atrazine
	Heptachlor	¹³ C ₁₀ Heptachlor*	¹³ C ₆ Alachlor
	Aldrin	¹³ C ₁₂ Aldrin*	¹³ C ₆ Alachlor
	Isodrin	¹³ C ₁₂ Aldrin*	¹³ C ₆ Alachlor
	Heptachlor epoxide	¹³ C ₁₀ Heptachlor epoxide*	¹³ C ₆ Alachlor
	trans-Chlordane	¹³ C ₁₀ trans-Chlordane*	¹³ C ₆ Alachlor
	cis-Chlordane	¹³ C ₁₀ trans-Chlordane*	¹³ C ₆ Alachlor
	2,4'-DDE	¹³ C ₁₂ 4,4'-DDE*	¹³ C ₆ Alachlor
	4,4'-DDE	¹³ C ₁₂ 4,4'-DDE*	¹³ C ₆ Alachlor
	α-Endosulfan	¹³ C ₁₀ trans-Nonachlor*	¹³ C ₆ Alachlor
	β-Endosulfan	¹³ C ₁₀ trans-Nonachlor*	¹³ C ₆ Alachlor
	Dieldrin	¹³ C ₁₂ Dieldrin*	¹³ C ₆ Alachlor
	Endrin	¹³ C ₁₂ Endrin*	¹³ C ₆ Alachlor
	2,4'-DDD	¹³ C ₁₂ 4,4'-DDD*	¹³ C ₆ Alachlor
	4,4'-DDD	¹³ C ₁₂ 4,4'-DDD*	¹³ C ₆ Alachlor
2,4'-DDT	¹³ C ₁₂ 4,4'-DDT*	¹³ C ₆ Alachlor	
4,4'-DDT	¹³ C ₁₂ 4,4'-DDT*	¹³ C ₆ Alachlor	

HCH = HexachloroCycloHexane; DDE = DichloroDiphenylDichloroEthylene; DDD = DichloroDiphenylDichloroethane; DDT = DichloroDiphenylTrichloroethane.

Table 3

High-resolution gas chromatograph/low-resolution mass spectrometer (HRGC/LRMS) operating conditions and instrumental parameters for PAHs determination.

HRGC/LRMS	Agilent Technologies 5973 inert Mass Selective Detector System
<i>Gas chromatographic separation</i>	
Column type	Agilent Technologies HP-5ms
Column length	30 m
Column I.D.	0.25 mm
Film thickness	0.25 μm
Carrier gas	Helium 5.5 (99.9995%)
Constant flow rate	0.8 mL min ⁻¹
Inlet mode	Splitless
Inlet temperature	300 °C
Oven	From 70 °C (holding time of 1.5 min) to 190 °C at 10 °C min ⁻¹ (holding time of 3 min), then to 280 °C at 5 °C min ⁻¹ (holding time of 5.5 min), finally to 300 °C at 20 °C min ⁻¹ (holding time of 1 min)
Total run time	42 min
Post run	18 min at 305 °C
Calibration compound	PFTBA (PerFluoroTriButylAmine)
<i>Mass spectrometer conditions</i>	
Source	Electron Ionization (EI), 70 eV
Source temperature	230 °C
Analyzer	Single quadrupole
Analyzer temperature	150 °C
Transfer line temperature	300 °C

Table 4

High-resolution gas chromatograph/low-resolution mass spectrometer (HRGC/LRMS) operating conditions and instrumental parameters for PCBs determination.

HRGC/LRMS	Agilent Technologies 5973 inert Mass Selective Detector System
<i>Gas chromatographic separation</i>	
Column type	Agilent Technologies HP-5ms
Column length	30 m
Column I.D.	0.25 mm
Film thickness	0.25 μm
Carrier gas	Helium 5.5 (99.9995%)
Constant flow rate	0.8 mL min ⁻¹
Inlet mode	Splitless
Inlet temperature	260 °C
Oven	From 90 °C (holding time of 3 min) to 160 °C at 20 °C min ⁻¹ , then to 260 °C at 3 °C min ⁻¹ (holding time of 4 min)
Total run time	44 min
Post run	1 min at 305 °C
Calibration compound	PFTBA (PerFluoroTriButylAmine)
<i>Mass spectrometer conditions</i>	
Source	Electron Ionization (EI), 70 eV
Source temperature	230 °C
Analyzer	Single quadrupole
Analyzer temperature	150 °C
Transfer line temperature	260 °C

Table 5

High-resolution gas chromatograph/high-resolution mass spectrometer (HRGC/HRMS) operating conditions and instrumental parameters for PBDEs determination.

HRGC/HRMS	Thermo Fisher Scientific MAT 95 XP
<i>Gas chromatographic separation</i>	
Column type	Agilent Technologies HP-5ms
Column length	15 m
Column I.D.	0.25 mm
Film thickness	0.25 μm
Carrier gas	Helium 5.5 (99.9995%)
Constant flow rate	1.0 mL min ⁻¹
Inlet mode	Splitless
Inlet temperature	290 °C
Oven	From 100 °C (holding time of 2 min) to 255 °C at 19 °C min ⁻¹ (holding time of 2 min), then to 310 °C at 20 °C min ⁻¹ (holding time of 5)
Total run time	20 min
Post run	10 min at 310 °C
Calibration compound	PFK (PerFluoroKerosene)
<i>Mass spectrometer conditions</i>	
Source	Electron Ionization (EI), 45 eV
Source temperature	290 °C
Analyzer	Double-focusing (magnetic and electric sectors)
Transfer line temperature	295 °C

Table 6

High-resolution gas chromatograph/low-resolution mass spectrometer (HRGC/LRMS) operating conditions and instrumental parameters for OCPs determination.

HRGC/LRMS	Agilent Technologies 5973 inert Mass Selective Detector System
<i>Gas chromatographic separation</i>	
Column type	Agilent Technologies HP-5ms
Column length	30 m
Column I.D.	0.25 mm
Film thickness	0.25 μm
Carrier gas	Helium 5.5 (99.9995%)
Constant flow rate	1.2 mL min ⁻¹
Inlet mode	Split (20:1)
Inlet temperature	290 °C
Oven	From 75 °C (holding time of 1 min) to 100 °C at 25 °C min ⁻¹ , then to 225 °C at 6 °C min ⁻¹ (holding time of 1 min), finally to 255 °C at 6 °C min ⁻¹ (holding time of 1 min)
Total run time	30 min
Post run	10 min at 310 °C
Calibration compound	PFTBA (PerFluoroTriButylAmine)
<i>Mass spectrometer conditions</i>	
Source	Electron Ionization (EI), 70 eV
Source temperature	230 °C
Analyzer	Single quadrupole
Analyzer temperature	150 °C
Transfer line temperature	290 °C

Table 7

Class of chlorination, congener number, and IUPAC (International Union of Pure And Applied Chemistry) name of the 21 analyzed PCBs.

Class of chlorination	Congener number	IUPAC name
Di-CB	11	3,3'-Dichlorobiphenyl
Tri-CB	28 ^a	2,4,4'-Trichlorobiphenyl
	29	2,4,5-Trichlorobiphenyl
Tetra-CB	52	2,2',5,5'-Tetrachlorobiphenyl
	77	3,3',4,4'-Tetrachlorobiphenyl
	81	3,4,4',5-Tetrachlorobiphenyl
Penta-CB	101 ^b	2,2',4,5,5'-Pentachlorobiphenyl
	105	2,3,3',4,4'-Pentachlorobiphenyl
	114	2,3,4,4',5-Pentachlorobiphenyl
	118	2,3',4,4',5-Pentachlorobiphenyl
	123	2,3',4,4',5'-Pentachlorobiphenyl
126	3,3',4,4',5-Pentachlorobiphenyl	
Hexa-CB	138 ^c	2,2',3,4,4',5'-Hexachlorobiphenyl
	153	2,2',4,4',5,5'-Hexachlorobiphenyl
	156	2,3,3',4,4',5-Hexachlorobiphenyl
	157	2,3,3',4,4',5'-Hexachlorobiphenyl
	167 ^d	2,3',4,4',5,5'-Hexachlorobiphenyl
169	3,3',4,4',5,5'-Hexachlorobiphenyl	
Hepta-CB	180	2,2',3,4,4',5,5'-Heptachlorobiphenyl
	185	2,2',3,4,5,5',6-Heptachlorobiphenyl
	189	2,3,3',4,4',5,5'-Heptachlorobiphenyl

^a Calculated as the sum of CB-28 and CB-31 (2,4',5-Trichlorobiphenyl);

^b Calculated as the sum of CB-90 (2,2',3,4',5-Pentachlorobiphenyl) and CB-101;

^c Calculated as the sum of CB-138 and CB-164 (2,3,3',4',5',6-Hexachlorobiphenyl);

^d Calculated as the sum of CB-128 (2,2',3,3',4,4'-Hexachlorobiphenyl) and CB-167.

Table 8

Class of bromination, congener number, and IUPAC (International Union of Pure and Applied Chemistry) name of the 14 analyzed PBDEs.

Class of bromination	Congener number	IUPAC name
Tri-BDE	17	2,2',4-Tribromodiphenyl ether
	28	2,4,4'-Tribromodiphenyl ether
Tetra-BDE	47	2,2',4,4'-Tetrabromodiphenyl ether
	66	2,3',4,4'-Tetrabromodiphenyl ether
	71	2,3',4',6-Tetrabromodiphenyl ether
Penta-BDE	85	2,2',3,3',6-Pentabromodiphenyl ether
	99	2,2',4,4',5-Pentabromodiphenyl ether
	100	2,2',4,4',6-Pentabromodiphenyl ether
Hexa-BDE	138	2,2',3,4,4',5'-Hexabromodiphenyl ether
	153	2,2',4,4',5,5'-Hexabromodiphenyl ether
	154	2,2',4,4',5,6'-Hexabromodiphenyl ether
Hepta-BDE	183	2,2',3,4,4',5',6-Heptabromodiphenyl ether
	190	2,3,3',4,4',5,6-Heptabromodiphenyl ether
Deca-BDE	209	Decabromodiphenyl ether

Table 9Concentrations (in ng g⁻¹) of the 15 analyzed PAHs. Method Detection Limits (MDLs; in ng g⁻¹) are also reported.

Core		CAV-04										CAV-06										MDLs
Level (cm)		1-2	2-3	4-5	5-6	6-7	15-16	21-22	29-30	34-35	49-50	0-1	4.5-6	6-7	7.5-8.5	9.5-10.5	18.5-19.5	27.5-28.5	31-32	48-50	61-62	
PAHs	Ac	b.d.l.	b.d.l.	6.06	b.d.l.	b.d.l.	b.d.l.	b.d.l.	b.d.l.	b.d.l.	b.d.l.	b.d.l.	b.d.l.	b.d.l.	b.d.l.	b.d.l.	b.d.l.	b.d.l.	b.d.l.	b.d.l.	b.d.l.	5.28
	Ace	17.8	b.d.l.	1.28	0.737	1.40	b.d.l.	b.d.l.	b.d.l.	b.d.l.	b.d.l.	b.d.l.	b.d.l.	b.d.l.	b.d.l.	b.d.l.	b.d.l.	b.d.l.	0.863	1.69	b.d.l.	0.629
	Flu	12.2	6.92	8.13	8.18	15.8	7.00	b.d.l.	4.05	b.d.l.	4.30	3.65	3.51	b.d.l.	4.76	b.d.l.	3.43	2.47	3.36	2.91	b.d.l.	1.50
	Phe	81.7	68.3	58.3	62.2	49.8	66.4	b.d.l.	50.5	13.4	34.0	b.d.l.	b.d.l.	17.8	56.6	b.d.l.	13.2	21.1	36.2	24.2	b.d.l.	10.8
	An	b.d.l.	b.d.l.	b.d.l.	b.d.l.	b.d.l.	1.84	b.d.l.	b.d.l.	b.d.l.	b.d.l.	b.d.l.	b.d.l.	b.d.l.	b.d.l.	b.d.l.	b.d.l.	b.d.l.	b.d.l.	3.65	b.d.l.	1.58
	Fluo	12.9	9.83	13.0	8.32	13.6	10.3	18.0	b.d.l.	b.d.l.	b.d.l.	b.d.l.	b.d.l.	4.08	14.4	5.32	4.70	14.7	5.10	19.3	8.46	3.94
	Pyr	8.10	6.50	16.2	b.d.l.	16.4	7.72	12.2	b.d.l.	b.d.l.	b.d.l.	b.d.l.	b.d.l.	b.d.l.	15.3	b.d.l.	b.d.l.	14.1	5.83	21.2	10.4	5.44
	B[a]An	2.00	2.55	3.09	1.68	3.30	3.86	5.80	b.d.l.	b.d.l.	b.d.l.	0.971	1.74	1.55	3.46	2.80	3.03	5.22	1.21	8.36	3.90	0.450
	Chr	8.48	9.66	12.3	9.74	14.4	17.6	19.7	b.d.l.	b.d.l.	b.d.l.	4.28	8.28	4.98	12.4	10.7	11.3	19.6	5.47	34.8	17.6	1.72
	B[b]Fluo	5.33	9.39	11.2	9.25	13.1	24.9	34.4	b.d.l.	b.d.l.	b.d.l.	4.85	5.14	2.41	11.8	7.66	11.9	23.2	6.23	37.5	14.4	1.12
	B[k]Fluo	b.d.l.	b.d.l.	b.d.l.	b.d.l.	b.d.l.	b.d.l.	2.48	b.d.l.	b.d.l.	3.30	11.4	13.1	2.64	3.52	4.66	7.30	2.12	2.97	5.86	b.d.l.	1.67
	B[a]Pyr	5.15	4.70	4.71	4.40	6.53	9.94	10.7	b.d.l.	b.d.l.	5.10	5.48	5.84	4.49	8.51	6.05	6.61	11.2	4.18	18.3	7.44	2.65
	B[ghi]Per	4.78	3.75	b.d.l.	b.d.l.	8.13	18.9	34.6	b.d.l.	b.d.l.	b.d.l.	b.d.l.	b.d.l.	b.d.l.	6.88	6.00	10.9	14.6	b.d.l.	25.2	7.15	0.006*
	I[123-cd]Pyr	6.19	2.63	6.56	3.38	5.63	15.7	30.3	b.d.l.	b.d.l.	b.d.l.	3.82	b.d.l.	2.40	9.44	5.04	7.53	9.83	2.81	19.1	4.65	1.78
	D[ah]An	b.d.l.	b.d.l.	b.d.l.	b.d.l.	b.d.l.	b.d.l.	2.79	b.d.l.	b.d.l.	b.d.l.	b.d.l.	b.d.l.	b.d.l.	b.d.l.	0.988	b.d.l.	1.72	b.d.l.	b.d.l.	b.d.l.	0.006*
	Σ ₁₅ PAHs	165	124	141	108	148	184	171	54.6	13.4	46.7	34.5	37.6	40.4	147	49.3	79.8	140	74.3	222	74.0	

* = Instrumental Detection Limit (IDL; no detectable peaks were found in the procedural blanks); b.d.l. = below the detection limit. Ac = Acenaphthylene; Ace = Acenaphthene; Flu = Fluorene; Phe = Phenanthrene; An = Anthracene; Fluo = Fluoranthene; Pyr = Pyrene; B[a]An = Benz[a]anthracene; Chr = Chrysene; B[b]Fluo = Benzo[b]fluoranthene; B[k]Fluo = Benzo[k]fluoranthene; B[a]Pyr = Benzo[a]pyrene; B[ghi]Per = Benzo[ghi]perylene; I[123-cd]Pyr = Indeno[1,2,3-cd]pyrene; D[ah]An = Dibenzo[a,h]anthracene.

Table 10Concentrations (in ng g⁻¹) of the 21 analyzed PCBs. Method Detection Limits (MDLs; in ng g⁻¹) are also reported.

Core		CAV-04										CAV-06										MDLs
Level (cm)		1-2	2-3	4-5	5-6	6-7	15-16	21-22	29-30	34-35	49-50	0-1	4.5-6	6-7	7.5-8.5	9.5-10.5	18.5-19.5	27.5-28.5	31-32	48-50	61-62	
PCBs	CB-11	1.60	1.14	1.27	0.811	1.01	3.58	7.71	0.642	0.419	7.00	0.395	0.419	0.374	1.05	0.204	0.482	3.64	0.815	6.64	1.32	0.0002*
	CB-29	b.d.l.	b.d.l.	b.d.l.	b.d.l.	b.d.l.	b.d.l.	b.d.l.	b.d.l.	b.d.l.	b.d.l.	b.d.l.	b.d.l.	b.d.l.	b.d.l.	b.d.l.	b.d.l.	b.d.l.	b.d.l.	0.117	b.d.l.	0.0002*
	CB-31,28	b.d.l.	0.552	0.865	0.562	0.816	5.86	1.22	0.377	0.349	1.68	0.293	0.232	0.513	0.779	b.d.l.	0.290	2.01	0.793	23.8	5.45	0.0001*
	CB-52	0.195	0.103	0.246	0.143	0.244	1.71	0.437	0.071	0.087	1.06	0.076	b.d.l.	b.d.l.	0.183	0.072	0.107	0.799	0.144	6.47	1.78	0.049
	CB-81	b.d.l.	b.d.l.	b.d.l.	b.d.l.	0.134	0.178	b.d.l.	b.d.l.	b.d.l.	b.d.l.	b.d.l.	b.d.l.	b.d.l.	0.152	b.d.l.	b.d.l.	0.096	b.d.l.	0.530	0.181	0.0003*
	CB-77	b.d.l.	b.d.l.	b.d.l.	b.d.l.	b.d.l.	1.64	0.424	b.d.l.	b.d.l.	1.24	b.d.l.	b.d.l.	b.d.l.	0.089	b.d.l.	b.d.l.	0.319	b.d.l.	2.33	0.670	0.0003*
	CB-101,90	0.284	0.170	0.365	0.348	0.333	3.03	0.894	0.097	0.183	1.34	0.107	0.096	0.064	0.355	0.184	0.316	1.32	0.257	6.92	1.72	0.005
	CB-123	b.d.l.	b.d.l.	b.d.l.	b.d.l.	b.d.l.	b.d.l.	b.d.l.	b.d.l.	b.d.l.	0.785	b.d.l.	b.d.l.	b.d.l.	b.d.l.	b.d.l.	b.d.l.	b.d.l.	b.d.l.	0.283	0.031	0.0004*
	CB-118	0.059	0.061	0.105	0.141	0.143	1.46	0.292	b.d.l.	b.d.l.	0.671	0.075	0.033	0.044	0.108	0.079	0.111	0.510	0.061	2.66	0.578	0.0003*
	CB-114	b.d.l.	b.d.l.	b.d.l.	b.d.l.	b.d.l.	0.159	b.d.l.	b.d.l.	b.d.l.	1.18	b.d.l.	b.d.l.	b.d.l.	b.d.l.	b.d.l.	b.d.l.	b.d.l.	b.d.l.	0.339	0.077	0.0004*
	CB-105	b.d.l.	b.d.l.	b.d.l.	0.168	0.270	2.20	0.290	b.d.l.	b.d.l.	1.17	b.d.l.	0.108	b.d.l.	0.245	0.185	0.259	0.824	0.254	4.08	0.974	0.0005*
	CB-126	b.d.l.	b.d.l.	b.d.l.	b.d.l.	b.d.l.	b.d.l.	b.d.l.	b.d.l.	b.d.l.	0.810	b.d.l.	b.d.l.	b.d.l.	b.d.l.	b.d.l.	b.d.l.	b.d.l.	b.d.l.	b.d.l.	b.d.l.	0.002*
	CB-153	b.d.l.	0.047	0.101	0.075	0.156	1.71	0.382	0.017	b.d.l.	0.667	0.056	0.049	0.077	0.087	0.080	0.183	0.797	0.072	2.81	0.692	0.003
	CB-164,138	0.057	0.072	0.149	0.101	0.215	2.31	0.530	0.019	0.031	1.28	0.076	0.030	0.045	0.148	0.112	0.234	1.08	0.093	3.94	0.875	0.004
	CB-128,167	b.d.l.	b.d.l.	b.d.l.	b.d.l.	0.118	1.09	0.258	b.d.l.	b.d.l.	1.82	b.d.l.	0.006	b.d.l.	b.d.l.	b.d.l.	0.134	0.408	b.d.l.	1.82	0.422	0.0006*
	CB-156	b.d.l.	b.d.l.	b.d.l.	b.d.l.	0.073	0.719	0.218	b.d.l.	b.d.l.	0.931	b.d.l.	0.029	b.d.l.	b.d.l.	b.d.l.	0.089	0.225	b.d.l.	1.02	0.217	0.001*
	CB-157	b.d.l.	b.d.l.	b.d.l.	b.d.l.	0.081	0.269	0.103	b.d.l.	b.d.l.	1.11	b.d.l.	0.042	b.d.l.	b.d.l.	b.d.l.	0.063	0.082	b.d.l.	0.269	0.072	0.0007*
	CB-169	b.d.l.	b.d.l.	b.d.l.	b.d.l.	b.d.l.	b.d.l.	b.d.l.	b.d.l.	b.d.l.	1.51	b.d.l.	b.d.l.	b.d.l.	b.d.l.	b.d.l.	b.d.l.	b.d.l.	b.d.l.	b.d.l.	b.d.l.	0.0006*
	CB-185	b.d.l.	b.d.l.	b.d.l.	b.d.l.	b.d.l.	0.040	0.015	b.d.l.	b.d.l.	0.492	b.d.l.	b.d.l.	b.d.l.	b.d.l.	b.d.l.	b.d.l.	0.023	b.d.l.	0.112	0.028	0.0003*
	CB-180	0.042	0.037	0.077	0.042	0.090	1.16	0.298	b.d.l.	b.d.l.	0.724	0.035	0.024	0.016	0.069	0.069	0.122	0.454	0.034	1.80	0.413	0.001*
	CB-189	b.d.l.	b.d.l.	b.d.l.	b.d.l.	b.d.l.	0.079	b.d.l.	b.d.l.	b.d.l.	0.889	b.d.l.	b.d.l.	b.d.l.	b.d.l.	b.d.l.	b.d.l.	0.030	b.d.l.	0.100	0.050	0.003*
Σ ₂₁ PCBs	2.23	2.18	3.18	2.39	3.68	27.2	13.1	1.22	1.07	26.4	1.11	1.07	1.13	3.26	0.985	2.39	12.6	2.52	66.1	15.5		

* = Instrumental Detection Limit (IDL; no detectable peaks were found in the procedural blanks); b.d.l. = below the detection limit.

Table 11
Concentrations (in ng g⁻¹) of the 14 analyzed PBDEs. Method Detection Limits (MDLs; in ng g⁻¹) are also reported.

Core		CAV-04										CAV-06											
		1-2	2-3	4-5	5-6	6-7	15-16	21-22	29-30	34-35	49-50	0-1	4.5-6	6-7	7.5-8.5	9.5-10.5	18.5-19.5	27.5-28.5	31-32	48-50	61-62	MDLs	
PBDEs	BDE-17	0.133	0.355	0.608	0.258	0.591	0.222	0.265	0.188	0.144	0.147	0.055	0.068	0.173	0.391	0.012	0.049	0.060	0.201	0.045	0.024	0.011	
	BDE-28	0.346	0.715	1.06	0.566	1.10	0.499	0.658	0.477	0.341	0.349	0.115	0.138	0.427	1.01	0.079	0.173	0.236	0.530	0.167	0.113	0.012	
	BDE-71	0.198	0.219	1.83	0.616	1.93	0.587	0.553	0.259	0.309	0.405	0.266	0.228	0.426	0.980	0.126	0.428	0.861	0.479	0.316	0.190	0.009	
	BDE-47	7.80	13.2	70.0	27.1	83.5	22.2	25.7	10.7	15.0	14.0	6.90	8.82	22.4	43.2	4.66	11.2	20.0	21.5	11.4	9.25	0.309	
	BDE-66	0.011	0.207	1.06	0.155	0.704	0.241	0.197	0.171	0.104	0.155	0.049	0.098	0.118	0.383	0.038	0.172	0.396	0.131	0.131	0.088	0.008	
	BDE-100	b.d.l.	0.319	2.50	1.89	2.16	1.41	1.08	0.367	0.413	0.506	0.453	0.488	0.614	1.13	0.276	0.594	0.834	0.539	0.521	0.705	0.076	
	BDE-99	0.305	1.43	6.54	5.65	5.27	3.96	2.67	1.17	1.31	1.41	2.16	2.67	1.94	3.48	1.33	2.17	2.79	1.94	2.12	3.33	0.148	
	BDE-85	b.d.l.	0.099	0.225	0.258	0.169	0.152	b.d.l.	b.d.l.	b.d.l.	b.d.l.	b.d.l.	b.d.l.	b.d.l.	b.d.l.	b.d.l.	b.d.l.	b.d.l.	b.d.l.	b.d.l.	b.d.l.	0.045	0.036
	BDE-154	b.d.l.	b.d.l.	b.d.l.	0.712	0.158	0.092	0.126	b.d.l.	b.d.l.	b.d.l.	0.066	b.d.l.	b.d.l.	b.d.l.	b.d.l.	b.d.l.	b.d.l.	b.d.l.	b.d.l.	b.d.l.	b.d.l.	0.066
	BDE-153	b.d.l.	0.268	1.63	0.578	0.419	0.171	0.138	b.d.l.	b.d.l.	0.127	b.d.l.	b.d.l.	b.d.l.	b.d.l.	b.d.l.	b.d.l.	b.d.l.	b.d.l.	b.d.l.	b.d.l.	b.d.l.	0.062
	BDE-138	b.d.l.	0.624	0.150	0.915	0.578	0.450	0.072	0.070	0.034	0.090	0.056	b.d.l.	b.d.l.	b.d.l.	b.d.l.	b.d.l.	b.d.l.	b.d.l.	b.d.l.	b.d.l.	b.d.l.	0.023
	BDE-183	b.d.l.	0.426	0.753	0.141	0.231	0.250	b.d.l.	b.d.l.	b.d.l.	0.147	b.d.l.	b.d.l.	b.d.l.	b.d.l.	b.d.l.	0.131	b.d.l.	b.d.l.	b.d.l.	b.d.l.	b.d.l.	0.076
	BDE-190	b.d.l.	b.d.l.	2.27	2.83	b.d.l.	0.415	0.504	b.d.l.	b.d.l.	b.d.l.	b.d.l.	b.d.l.	b.d.l.	b.d.l.	b.d.l.	b.d.l.	b.d.l.	b.d.l.	b.d.l.	b.d.l.	b.d.l.	0.346
	BDE-209	b.d.l.	b.d.l.	b.d.l.	b.d.l.	b.d.l.	b.d.l.	b.d.l.	b.d.l.	b.d.l.	b.d.l.	b.d.l.	b.d.l.	0.365	2.66	b.d.l.	b.d.l.	2.53	0.207	0.251	0.186	0.00004*	
Σ ₁₄ PBDEs	8.79	17.9	88.6	41.7	96.8	30.6	31.9	13.4	17.6	17.4	10.1	12.5	26.4	53.2	6.52	14.9	27.7	25.5	14.9	13.9			

* = Instrumental Detection Limit (IDL; no detectable peaks were found in the procedural blanks); b.d.l. = below the detection limit.

Table 12Concentrations (in ng g⁻¹) of the 22 analyzed OCPs. Method Detection Limits (MDLs; in ng g⁻¹) are also reported.

Core	CAV-04										CAV-06										MDLs	
	Level (cm)	1-2	2-3	4-5	5-6	6-7	15-16	21-22	29-30	34-35	49-50	0-1	4.5-6	6-7	7.5-8.5	9.5-10.5	18.5-19.5	27.5-28.5	31-32	48-50		61-62
OCPs	PeCB	1-2	2-3	4-5	5-6	6-7	15-16	21-22	29-30	34-35	49-50	0-1	4.5-6	6-7	7.5-8.5	9.5-10.5	18.5-19.5	27.5-28.5	31-32	48-50	61-62	0.003*
	HCB	1-2	2-3	4-5	5-6	6-7	15-16	21-22	29-30	34-35	49-50	0-1	4.5-6	6-7	7.5-8.5	9.5-10.5	18.5-19.5	27.5-28.5	31-32	48-50	61-62	0.002*
	α -HCH	b.d.l.	b.d.l.	b.d.l.	b.d.l.	b.d.l.	b.d.l.	b.d.l.	b.d.l.	b.d.l.	b.d.l.	b.d.l.	b.d.l.	b.d.l.	b.d.l.	b.d.l.	b.d.l.	b.d.l.	b.d.l.	b.d.l.	b.d.l.	0.045*
	β -HCH	b.d.l.	b.d.l.	b.d.l.	b.d.l.	b.d.l.	b.d.l.	b.d.l.	b.d.l.	b.d.l.	b.d.l.	b.d.l.	b.d.l.	b.d.l.	b.d.l.	b.d.l.	b.d.l.	b.d.l.	b.d.l.	b.d.l.	b.d.l.	0.062*
	γ -HCH	b.d.l.	b.d.l.	b.d.l.	b.d.l.	b.d.l.	b.d.l.	b.d.l.	b.d.l.	b.d.l.	b.d.l.	b.d.l.	b.d.l.	b.d.l.	b.d.l.	b.d.l.	b.d.l.	b.d.l.	b.d.l.	b.d.l.	b.d.l.	0.055*
	δ -HCH	b.d.l.	b.d.l.	b.d.l.	b.d.l.	b.d.l.	b.d.l.	b.d.l.	b.d.l.	b.d.l.	b.d.l.	b.d.l.	b.d.l.	b.d.l.	b.d.l.	b.d.l.	b.d.l.	b.d.l.	b.d.l.	b.d.l.	b.d.l.	0.007*
	HpC	b.d.l.	b.d.l.	b.d.l.	b.d.l.	b.d.l.	b.d.l.	b.d.l.	b.d.l.	b.d.l.	b.d.l.	b.d.l.	b.d.l.	b.d.l.	b.d.l.	b.d.l.	b.d.l.	b.d.l.	b.d.l.	b.d.l.	b.d.l.	0.039*
	ALD	b.d.l.	b.d.l.	b.d.l.	b.d.l.	b.d.l.	b.d.l.	b.d.l.	b.d.l.	b.d.l.	b.d.l.	b.d.l.	b.d.l.	b.d.l.	b.d.l.	b.d.l.	b.d.l.	b.d.l.	b.d.l.	b.d.l.	b.d.l.	0.005*
	ISD	b.d.l.	b.d.l.	b.d.l.	b.d.l.	b.d.l.	b.d.l.	b.d.l.	b.d.l.	b.d.l.	b.d.l.	b.d.l.	2.09	b.d.l.	b.d.l.	b.d.l.	b.d.l.	b.d.l.	b.d.l.	b.d.l.	b.d.l.	0.007*
	HpEX	23.9	4.10	b.d.l.	b.d.l.	b.d.l.	0.663	b.d.l.	b.d.l.	b.d.l.	b.d.l.	b.d.l.	0.779	b.d.l.	b.d.l.	b.d.l.	17.5	b.d.l.	1.94	6.94	b.d.l.	0.002*
	t-CLD	b.d.l.	b.d.l.	b.d.l.	b.d.l.	b.d.l.	b.d.l.	b.d.l.	b.d.l.	b.d.l.	b.d.l.	b.d.l.	b.d.l.	b.d.l.	b.d.l.	b.d.l.	b.d.l.	0.213	b.d.l.	b.d.l.	0.424	0.003*
	c-CLD	17.8	b.d.l.	b.d.l.	b.d.l.	b.d.l.	b.d.l.	12.0	b.d.l.	2.15	b.d.l.	b.d.l.	b.d.l.	b.d.l.	b.d.l.	b.d.l.	b.d.l.	b.d.l.	b.d.l.	b.d.l.	b.d.l.	1.134
	24E	b.d.l.	b.d.l.	b.d.l.	b.d.l.	b.d.l.	b.d.l.	b.d.l.	b.d.l.	b.d.l.	b.d.l.	b.d.l.	b.d.l.	b.d.l.	b.d.l.	b.d.l.	b.d.l.	b.d.l.	b.d.l.	b.d.l.	b.d.l.	0.007*
	44E	0.913	b.d.l.	b.d.l.	b.d.l.	b.d.l.	b.d.l.	0.404	b.d.l.	b.d.l.	b.d.l.	b.d.l.	b.d.l.	b.d.l.	b.d.l.	b.d.l.	b.d.l.	1.16	b.d.l.	b.d.l.	0.843	0.024*
	α -EDS	b.d.l.	b.d.l.	b.d.l.	b.d.l.	b.d.l.	b.d.l.	b.d.l.	b.d.l.	b.d.l.	b.d.l.	b.d.l.	b.d.l.	b.d.l.	b.d.l.	b.d.l.	b.d.l.	b.d.l.	b.d.l.	b.d.l.	b.d.l.	0.026*
	β -EDS	b.d.l.	b.d.l.	b.d.l.	b.d.l.	b.d.l.	b.d.l.	b.d.l.	b.d.l.	b.d.l.	b.d.l.	b.d.l.	4.27	b.d.l.	b.d.l.	b.d.l.	b.d.l.	b.d.l.	b.d.l.	b.d.l.	b.d.l.	0.025*
	DLD	b.d.l.	b.d.l.	b.d.l.	b.d.l.	b.d.l.	b.d.l.	b.d.l.	b.d.l.	b.d.l.	b.d.l.	b.d.l.	b.d.l.	b.d.l.	b.d.l.	b.d.l.	b.d.l.	b.d.l.	b.d.l.	b.d.l.	b.d.l.	0.005*
	END	b.d.l.	b.d.l.	b.d.l.	b.d.l.	b.d.l.	b.d.l.	b.d.l.	b.d.l.	b.d.l.	b.d.l.	b.d.l.	b.d.l.	b.d.l.	b.d.l.	b.d.l.	b.d.l.	b.d.l.	b.d.l.	b.d.l.	b.d.l.	0.008*
	24D	6.02	b.d.l.	b.d.l.	b.d.l.	b.d.l.	b.d.l.	b.d.l.	b.d.l.	b.d.l.	b.d.l.	b.d.l.	b.d.l.	b.d.l.	b.d.l.	b.d.l.	b.d.l.	b.d.l.	b.d.l.	b.d.l.	b.d.l.	0.002*
	44D	b.d.l.	b.d.l.	b.d.l.	b.d.l.	b.d.l.	b.d.l.	b.d.l.	b.d.l.	b.d.l.	b.d.l.	b.d.l.	b.d.l.	b.d.l.	b.d.l.	b.d.l.	b.d.l.	b.d.l.	b.d.l.	b.d.l.	b.d.l.	0.002*
	24T	175	b.d.l.	b.d.l.	b.d.l.	b.d.l.	b.d.l.	132	b.d.l.	74.0	b.d.l.	b.d.l.	b.d.l.	b.d.l.	b.d.l.	b.d.l.	b.d.l.	b.d.l.	b.d.l.	b.d.l.	b.d.l.	15.21
	44T	27.4	b.d.l.	b.d.l.	b.d.l.	b.d.l.	b.d.l.	b.d.l.	b.d.l.	b.d.l.	b.d.l.	b.d.l.	b.d.l.	b.d.l.	b.d.l.	b.d.l.	b.d.l.	b.d.l.	b.d.l.	b.d.l.	b.d.l.	0.005*
	Σ_{22} OCPs	255	4.10	b.d.l.	b.d.l.	b.d.l.	0.663	145	b.d.l.	76.1	b.d.l.	b.d.l.	8.17	b.d.l.	b.d.l.	b.d.l.	17.5	1.37	1.94	6.94	2.39	

* = Instrumental Detection Limit (IDL; no detectable peaks were found in the procedural blanks); b.d.l. = below the detection limit.

PeCB = Pentachlorobenzene; HCB = Hexachlorobenzene; HCH = HexachloroCycloHexane; HpC = Heptachlor; ALD = Aldrin; ISD = Isodrin; HpEX = Heptachlor epoxide; t-CLD = trans-Chlordane; c-CLD = cis-Chlordane; 24E = 2,4'-DDE (DichloroDiphenylDichloroEthylene); 44E = 4,4'-DDE; EDS = Endosulfan; DLD = Dieldrin; END = Endrin; 24D = 2,4'-DDD (DichloroDiphenylDichloroethane); 44D = 4,4'-DDD; 24T = 2,4'-DDT (DichloroDiphenylTrichloroethane); 44T = 4,4'-DDT.

2. Experimental Design, Materials and Methods

The Lake of Cavazzo is a natural lacustrine basin in the Friuli Venezia Giulia Region (NE Italy) that occupies a fluvio-glacial valley of the Tagliamento River, at the Southern front of the alpine chain (Fig. 1a). It is located in a seismically active region within the Eurasia-Adria collision zone where strong earthquakes have been reported since medieval times [4].

The lake has sustained substantial environmental and physiographic changes in the last decades, principally following the urbanization of the area and the construction of industrial and transport infrastructures (Fig. 1b). The Somplago hydroelectric power plant was built in 1953–1958 on the Northern shores of the lake and, since then, has discharged there its drainage waters and sediments [5]. In 1980, the 7-year long construction of the A23 highway viaduct was completed, leaving an evident mark on the lake catchment area [5]. In the meantime, the lake suffered a major flood of the Tagliamento River in 1966, and a sequence of large magnitude earthquakes in 1976–1977. These catastrophic events were among the strongest ever recorded in Northern Italy, and caused many casualties and destruction in the lake valley [6].

The present work has originated from the request by local administrations and associations to try to find the causes for the observed decline in the environmental quality of the lake. Previous multi-proxy studies of dated sediment cores [2,3] were able to reconstruct the major changes of the last century and evidenced the impact of these natural/anthropogenic events on the lake sedimentary system. However they did not focus on the definition of varying organic pollutant inputs during the same time frame, that might be associated with specific anthropogenic impacts. Data from the present work can help fill this gap for PAHs, PCBs, PBDEs, and OCPs, based on stratigraphic interpretation and data from Polonia et al. [2,3].

Cores CAV-04 and CAV-06 were collected using a small boat equipped with a water/sediment gravity corer hosting a 6 cm diameter plastic liner, during a first geological/geophysical survey in May 2015 (Fig. 1c and d). Core CAV-06 was collected close to the lake depocenter (Fig. 1a), while core CAV-04 was collected close to the lake's Southern borders (Fig. 1a). The two core locations were selected in order to acquire information relative to two different aspects: (1) the overall status of contamination for the analyzed chemicals averaged over the entire lake basin, as can be observed in locations close to the depocenter which collect inputs from all over the lake (CAV-06); (2) the presence of local/small scale inputs that affect predominantly limited areas of the lake but are nevertheless very meaningful when trying to assess the managing options for recovery (core CAV-04). Core profiles could provide information on an annual-multiannual seasonal scale, seasonal variations being beyond our analytical resolution.

The cores were opened in half (Fig. 1e and f) and described through visual investigations and color photos. Sediment radiochronology was acquired using ^{210}Pb and ^{137}Cs radioisotopes (Fig. 2). Data were coupled to laminae counting to provide a multi-tracer evaluation of sediment ages and accumulation rates (Fig. 2), as described in Polonia et al. [2,3]. During the horizontal scans of an Avaatech XRF Core Scanner, high resolution pictures were taken and the relative transformation as numeric RGB color code was obtained (Fig. 3).

Samples for the analyzes of PAHs, PCBs, PBDEs, and OCPs were selected in order to have at least one measurement in each of the three main sedimentary units (Fig. 3). When possible, samples belonging to the most recent Unit A were collected at levels representative of both oxic and anoxic conditions, these latter resulting from the impact of episodic hyperepycnal discharges from the Somplago hydroelectric power plant [2]. Details are provided in Table 1. Sediments were collected from the center of the core and far from its borders, in order to avoid any contamination from the plastic liners and cross-contamination between different sediment layers. This is something that can happen when the corer sneaks in the bottom sediments and is subsequently brought back on board. In addition, all tools and glassware were washed with an aqueous 2% (v/v) Contrad[®] 2000 solution (VWR International), dried, and rinsed three times with dichloromethane and three times with *n*-hexane. PAHs, PCBs, PBDEs, and OCPs were determined with the same sample preparation protocol, built up with reference both to United States Environmental Protection Agency (US EPA) and other literature methods [7] for the si-

multaneous determination of PAHs and different classes of Persistent Organic Pollutants (POPs) in varying environmental matrices [8–11]. The sample amount and the operative conditions were optimized to enhance extraction efficiency and minimize the volume of solvent required.

The extraction of analytes was performed with an ASETM 350 system (Accelerated Solvent Extractor; Thermo Fisher Scientific Dionex) equipped with stainless steel extraction cells, supported with stainless steel end caps and filters. Before extraction, procedural blanks and samples were spiked with a known amount of a ¹³C isotope-labeled standard solution (3 ¹³C-labeled PAHs at 1 ng μL^{-1} ; 17 ¹³C-labeled PCBs at 40 pg μL^{-1} ; 8 ¹³C-labeled PBDEs at 20–200 pg μL^{-1} ; 14 ¹³C-labeled OCPs at 50 pg μL^{-1} ; Table 2). About 0.3–0.5 g of the homogenized sub-samples of freeze-dried sediment were mixed with diatomaceous earth (Applied Separations) as dispersing agent and anhydrous sodium sulfate (Sigma-Aldrich) to remove humidity, then placed in a 22 mL cell, spiked, and covered with Ottawa sand (Applied Separations). Analyte extractions were carried out at 100 bar and 100 °C in three cycles of 5 min each, using *n*-hexane-dichloromethane (1:1; v/v) as extracting solvent.

To remove elemental sulfur from samples, the extracts were eluted through activated metallic copper (Sigma-Aldrich), then reduced to 500 μL under a gentle 5.0 (99.999% of purity) nitrogen flow at 23 °C (Turbovap[®] II; Caliper Life Science).

The samples were then made up to 2 mL with *n*-hexane to change solvent and transferred into a glass syringe for injection into the automated clean-up system Power-PrepTM (FMS – Fluid Management System). Extract clean-up was performed by directly injecting the sample into a disposable neutral silica column (19.5 cm \times 0.9 cm with 6 g of silica; FMS) previously conditioned with 50 mL of *n*-hexane. Elution was carried out with 30 mL of *n*-hexane followed by 30 mL of *n*-hexane-dichloromethane (1:1; v/v). The eluates were collected as one single fraction.

Before instrumental analysis, the volume of each purified sample was reduced to 100 μL and spiked with a known amount of a recovery standard solution containing ¹³C₆-Chrysene at 1 ng μL^{-1} ; ¹³C₁₂-CB-47 and ¹³C₁₂-CB-141 at 40 pg μL^{-1} ; ¹³C₁₂-BDE-77 and ¹³C₁₂-BDE-126 at 10–15 pg μL^{-1} ; ¹³C₆-Alachlor and ¹³C₃-Atrazine at 100 pg μL^{-1} (Table 2). The different steps of the analytical procedure for the analyses of PAHs, PCBs, PBDEs, and OCPs are shown as a flow chart in Fig. 4.

Instrumental determination of PAHs, PCBs, and OCPs was carried out with a single-quadrupole Low-Resolution Mass Spectrometer (LRMS) Agilent Technologies 5973 inert Mass Selective Detector System, operating in Electron Ionization mode (EI), coupled with a Gas Chromatograph (GC) Hewlett Packard - Agilent Technologies 6890 Series GC System, equipped with an Agilent Technologies HP5-ms column (30 m, 0.25 mm I.D., 0.25 μm film thickness). Acquisition was performed using Selected Ion Monitoring (SIM) mode, while quantification was performed using internal standards and the isotopic dilution technique, employing PerFluoroTriButylAmine (PFTBA) as the calibration compound.

Instrumental determination of PBDEs was carried out with a double-focusing High-Resolution Mass Spectrometer (HRMS) Thermo Fisher Scientific MAT 95 XP, operating in EI mode, coupled with a GC of the same type but equipped with a shorter Agilent Technologies HP5-ms column (15 versus 30 m, 0.25 mm I.D., 0.25 μm film thickness), thus avoiding the decomposition of high-brominated congeners (i.e. BDE-209) before their detection [9,12–14]. Acquisition was performed using Multiple Ion Detection (MID) mode, while quantification was performed using internal standards and the isotopic dilution technique, employing PerFluoroKerosene (PFK) as the calibration compound. Experiments were carried out monitoring the two most intense peaks of the EI spectra for each analyte.

Raw instrumental data were corrected using the instrumental response factors and subtracting the procedural blanks, and were calculated on a dry weight basis. Operating conditions and instrumental parameters are presented in Tables 3–6.

15 PAHs, 21 PCB congeners (including the non-Aroclor CB-11; Table 7), 14 PBDE congeners (Table 8), and 22 OCPs were investigated. Detected concentrations for all the 72 analytes considered are reported in Tables 9–12.

Precision, expressed as repeatability, was calculated as the Relative Standard Deviation (RSD%) of three replicated analyses each of two Standard Reference Materials (SRMs): SRM 1941a -

Organics in Marine Sediment (NIST – National Institute of Standards and Technology) and SRM SQC072 - *PBDE/PCBs in Soil* (RTC – R.T. Corporation). For PAHs, RSD% was 11% on average, ranging between 3.5 and 38% (Acenaphthene). For PCBs, it varied from 2.6 to 23% (CB-3128) with an average value of 8.2%. For PBDEs, RSD% was 4.8% on average and varied from a minimum of 2.1 to a maximum of 7.9%. For OCPs, it ranged from 0.4 to 20% with an average value of 7.2%.

Accuracy was estimated through the comparison of the values obtained from the analysis of the above-defined SRMs with their certified/reference values. It was expressed as average Relative Error (R_E), and was 0.28, 0.61, 0.34, and 0.13 for PAHs, PCBs, PBDEs, and OCPs, respectively.

For triplicate analysis, the mean recovery percentage was $92 \pm 6\%$ for PAHs, $88 \pm 13\%$ for PCBs, $73 \pm 31\%$ for PBDEs, and $61 \pm 8\%$ for OCPs.

Procedural blanks were used to determine the MDLs (ng g^{-1}) associated to the employed analytical methods. Data obtained from the analyses of three replicates allowed the definition of the average MDLs that are summarized in Tables 9–12. Where no detectable peaks were found in the blank, the Instrumental Detection Limit (IDL, ng g^{-1}) value was used in the determination of the DL.

Ethics Statements

None.

Declaration of Competing Interest

The authors declare that they have no known competing financial interests or personal relationships that could have appeared to influence the work reported in this paper.

Data Availability

Dataset of analyzes performed to determine the level and timing of selected organic pollutants' inputs in sediments of the Lake of Cavazzo (Italy) (Original data) (DIB).

CRediT Author Statement

Sarah Pizzini: Validation, Formal analysis, Investigation, Writing – original draft, Writing – review & editing; **Silvia Giuliani:** Conceptualization, Formal analysis, Writing – original draft, Writing – review & editing, Visualization; **Alina Polonia:** Conceptualization, Formal analysis, Writing – review & editing; **Rossano Piazza:** Resources, Writing – review & editing; **Luca Giorgio Bellucci:** Conceptualization, Writing – review & editing; **Beatrice Orlando:** Formal analysis; **Andrea Gambaro:** Resources; **Luca Gasperini:** Conceptualization, Writing – review & editing, Project administration, Funding acquisition.

Acknowledgments

The Municipality of Trasaghis supported the work in the field and funded part of the research. This is ISMAR-Bologna scientific contribution n. 2071.

References

- [1] S. Pizzini, S. Giuliani, A. Polonia, R. Piazza, L.G. Bellucci, A. Gambaro, L. Gasperini, PAHs, PCBs, PBDEs, and OCPs trapped and remobilized in the Lake of Cavazzo (NE Italy) sediments: temporal trends, quality, and sources in an area prone to anthropogenic and natural stressors, *Environ. Res.* 213 (2022) 113573, doi:10.1016/j.envres.2022.113573.

- [2] A. Polonia, S. Albertazzi, L.G. Bellucci, C. Bonetti, J. Bonetti, G. Giorgetti, S. Giuliani, M.L. Correa, C. Mayr, L. Peruzza, G. Stanghellini, L. Gasperini, Decoding a complex record of anthropogenic and natural impacts in the Lake of Cavazzo sediments, NE Italy. *Sci. Total Environ.* 787 (2021) 147659, doi:[10.1016/j.scitotenv.2021.147659](https://doi.org/10.1016/j.scitotenv.2021.147659).
- [3] A. Polonia, S. Albertazzi, L.G. Bellucci, C. Bonetti, J. Bonetti, A. Gallerani, G. Giorgetti, S. Giuliani, M.L. Correa, C. Mayr, S. Miserocchi, L. Peruzza, F. Savelli, G. Stanghellini, L. Gasperini, Multidisciplinary dataset for geological and environmental studies in the lake of Cavazzo (Southern Alps), *Data Brief* 37 (2021) 107202, doi:[10.1016/j.dib.2021.107202](https://doi.org/10.1016/j.dib.2021.107202).
- [4] A. Rovida, M. Locati, R. Camassi, B. Lolli, P. Gasperini, The Italian earthquake catalogue CPTI15, *Bull. Earthq. Eng.* 18 (2020) 2953–2984, doi:[10.1007/s10518-020-00818-y](https://doi.org/10.1007/s10518-020-00818-y).
- [5] P. Pironio, G. Dri, V. Rabassi, Condizioni fisiche del lago di Cavazzo o dei Tre Comuni, in: *Obiettivo lago Il lago di Cavazzo o dei Tre Comuni: un patrimonio da salvare e valorizzare. Proceedings of the Convegno Tecnico Scientifico, Alesso di Trasaghis, 12-13 September 1987, Treu Arti Grafiche, Tolmezzo (UD), Italy, 1989* In Italian.
- [6] M. Govi, Photo-interpretation and mapping of the landslides triggered by the Friuli earthquake (1976), *Bull. Int. Assoc. Eng. Geol.* 15 (1977) 67–72, doi:[10.1007/BF02592650](https://doi.org/10.1007/BF02592650).
- [7] R. Piazza, B. El Moumni, L.G. Bellucci, M. Frignani, M. Vecchiato, S. Giuliani, S. Romano, R. Zangrando, A. Gambaro, Polychlorinated biphenyls in sediments of selected coastal environments in northern Morocco, *Mar. Pollut. Bull.* 58 (3) (2009) 431–438, doi:[10.1016/j.marpolbul.2008.11.020](https://doi.org/10.1016/j.marpolbul.2008.11.020).
- [8] R. Piazza, A. Gambaro, E. Argiriadis, M. Vecchiato, S. Zambon, P. Cescon, C. Barbante, Development of a method for simultaneous analysis of PCDDs, PCDFs, PCBs, PBDEs, PCNs and PAHs in Antarctic air, *Anal. Bioanal. Chem.* 405 (2013) 917–932, doi:[10.1007/s00216-012-6464-y](https://doi.org/10.1007/s00216-012-6464-y).
- [9] S. Pizzini, E. Marchiori, R. Piazza, G. Cozzi, C. Barbante, Determination by HRGC/HRMS of PBDE levels in edible Mediterranean bivalves collected from north-western Adriatic coasts, *Microchem. J.* 121 (2015) 184–191, doi:[10.1016/j.microc.2015.03.010](https://doi.org/10.1016/j.microc.2015.03.010).
- [10] S. Pizzini, R. Piazza, G. Cozzi, C. Barbante, Simultaneous determination of halogenated contaminants and polycyclic aromatic hydrocarbons: a multi-analyte method applied to filter-feeding edible organisms, *Anal. Bioanal. Chem.* 408 (2016) 7991–7999, doi:[10.1007/s00216-016-9897-x](https://doi.org/10.1007/s00216-016-9897-x).
- [11] S. Pizzini, E. Morabito, E. Gregoris, M. Vecchiato, F. Corami, R. Piazza, A. Gambaro, Occurrence and source apportionment of organic pollutants in deep sediment cores of the Venice Lagoon, *Mar. Pollut. Bull.* 164 (2021) 112053, doi:[10.1016/j.marpolbul.2021.112053](https://doi.org/10.1016/j.marpolbul.2021.112053).
- [12] H.M. Stapleton, Instrumental methods and challenges in quantifying polybrominated diphenyl ethers in environmental extracts: a review, *Anal. Bioanal. Chem.* 386 (2006) 807–817, doi:[10.1007/s00216-006-0400-y](https://doi.org/10.1007/s00216-006-0400-y).
- [13] L. Webster, J. Tronczynski, P. Bersuder, K. Vorkamp, P. Lepom, Determination of polybrominated diphenyl ethers (PBDEs) in sediment and biota, *ICES Tech. Mar. Environ. Sci.* 46 (2010) 16 pages.
- [14] S. Giuliani, M. Romanelli, R. Piazza, M. Vecchiato, S. Pizzini, G. Tranchida, F. D'Agostino, S. Romano, L.G. Bellucci, When research meets NGOs: the GVC-UCODEP project in the Bắc Giang Province and Cầu River (Northern Vietnam) and its feedback on national monitoring programs, *Environ. Sci. Policy* 101 (2019) 279–290, doi:[10.1016/j.envsci.2019.09.004](https://doi.org/10.1016/j.envsci.2019.09.004).